Physica Medica (2013) 29, 357–367

Available online at www.sciencedirect.com

SciVerse ScienceDirect

journal homepage: http:// www.physicamedica.com

ORIGINAL PAPER

The use of non-standard CT conversion ramps for Monte Carlo verification of 6 MV prostate IMRT plans

M. Zarza-Moreno [a,b,*], I. Cardoso [c], N. Teixeira [d], A.P. Jesus [a,b], G. Mora [b]

[a] Faculdade de Ciências e Tecnologia, Universidade Nova de Lisboa, Portugal
[b] Centro de Física Nuclear, Universidade de Lisboa, Portugal
[c] CONC/Quadrantes – Medical Consult, Lisboa, Portugal
[d] Escola Superior de Tecnologia da Saúde de Lisboa, Portugal

Received 17 February 2012; received in revised form 7 May 2012; accepted 8 May 2012
Available online 6 June 2012

KEYWORDS
Monte Carlo algorithms;
IMRT;
CT conversion ramp;
Prostate cancer;
Pencil beam convolution algorithms

Abstract Monte Carlo (MC) dose calculation algorithms have been widely used to verify the accuracy of intensity-modulated radiotherapy (IMRT) dose distributions computed by conventional algorithms due to the ability to precisely account for the effects of tissue inhomogeneities and multileaf collimator characteristics. Both algorithms present, however, a particular difference in terms of dose calculation and report. Whereas dose from conventional methods is traditionally computed and reported as the water-equivalent dose (D_w), MC dose algorithms calculate and report dose to medium (D_m). In order to compare consistently both methods, the conversion of MC D_m into D_w is therefore necessary.

This study aims to assess the effect of applying the conversion of MC-based D_m distributions to D_w for prostate IMRT plans generated for 6 MV photon beams. MC phantoms were created from the patient CT images using three different ramps to convert CT numbers into material and mass density: a conventional four material ramp (CTCREATE) and two simplified CT conversion ramps: (1) air and water with variable densities and (2) air and water with unit density. MC simulations were performed using the BEAMnrc code for the treatment head simulation and the DOSXYZnrc code for the patient dose calculation. The conversion of D_m to D_w by scaling with the stopping power ratios of water to medium was also performed in a post-MC calculation process.

The comparison of MC dose distributions calculated in conventional and simplified (water with variable densities) phantoms showed that the effect of material composition on dose-volume histograms (DVH) was less than 1% for soft tissue and about 2.5% near and inside bone structures.

* Corresponding author. Centro de Física Nuclear da Universidade de Lisboa, Av. Prof. Gama Pinto 2, 1649 – 003 Lisbon, Portugal. Tel.: +351 217904812; fax: +351 217954288.
E-mail addresses: miriamzamo@gmail.com, miriam@cii.fc.ul.pt (M. Zarza-Moreno).

1120-1797/$ - see front matter
doi:10.1016/j.ejmp.2012.05.004

The effect of material density on DVH was less than 1% for all tissues through the comparison of MC distributions performed in the two simplified phantoms considering water. Additionally, MC dose distributions were compared with the predictions from an Eclipse treatment planning system (TPS), which employed a pencil beam convolution (PBC) algorithm with Modified Batho Power Law heterogeneity correction. Eclipse *PBC* and MC calculations (conventional and simplified phantoms) agreed well ($<$1%) for soft tissues. For femoral heads, differences up to 3% were observed between the DVH *for Eclipse PBC* and MC calculated in conventional phantoms. The use of the CT conversion ramp of water with variable densities for MC simulations showed no dose discrepancies (0.5%) with *the PBC algorithm*. Moreover, converting D_m to D_w using mass stopping power ratios resulted in a significant shift (up to 6%) in the DVH for the femoral heads compared to *the Eclipse PBC one*.

Our results show that, for prostate IMRT plans delivered with 6 MV photon beams, no conversion of MC dose from medium to water using stopping power ratio is needed. In contrast, MC dose calculations using water with variable density may be a simple way to solve the problem found using the dose conversion method based on the stopping power ratio.

Introduction

IMRT has rapidly become an effective technique for the treatment of prostate cancer because of the ability of delivering highly conformal dose distributions to tumor targets, reducing doses, especially, to the rectum [1]. The improved dose conformity achieved with the IMRT technique leads, however, to an increase of the complexity of the treatment, involving the use of small fields and large intensity dose gradients. Consequently, inaccuracies in the calculation algorithms may be introduced, magnifying the possible dosimetric errors caused by the presence of tissue inhomogeneities such as air cavities or bone tissues. Hence, a rigorous verification of the IMRT plans is required, in order to ensure the accurate determination of the absorbed dose before the treatment delivery [2].

Commonly, the direct measurements using ionization chambers and films in homogeneous phantoms are the widely used method for checking the IMRT dose distributions. Nevertheless, there are factors that may cause experimental data to be insufficient to completely characterize the IMRT dose distributions. On one side, it is known that the dosimeters present some limitations for IMRT fields, due to the presence of high dose gradient, small fields or dynamic beam delivery [3]. On the other side, the use of homogeneous phantoms as a medium to verify measurements cannot provide direct checks of the accuracy of the patient dose calculation, since they do not represent a true and heterogeneous patient geometry [4]. In contrast to the measurements, Monte Carlo dose algorithms have shown to be a more reliable tool to improve dose accuracy, in such situations due to the ability to model realistic radiation transport through the accelerator treatment head, multileaf collimators (MLCs) and patient-specific geometry with heterogeneities. Furthermore, in recent years, with the rapid development in computer technology, MC algorithms have been implemented for the dosimetric verification of IMRT plans generated from conventional treatment planning systems (TPS) [5–7].

It is well known that conventional dose calculation algorithms implemented in most of TPS, such as pencil beam or superposition/convolution algorithms, compute and report the absorbed dose to water (D_w), assuming that the majority of the patient body (between 45 and 75 %) consist of water [8]. Historically, measured and prescribed doses have been also reported in terms of D_w and modern dosimetry protocols have been also based on this consideration (AAPM TG-51 and IAEA 2000). In contrast, Monte Carlo dose calculation algorithms calculate and report the absorbed dose to medium (D_m). In fact, MC patient dose calculations can be performed in the explicit media of phantoms built from real patient CT (computed tomography) anatomical information.

With the use of MC algorithms as a tool to verify the dose accuracy computed by TPS conventional algorithms, it is therefore necessary to convert dose to medium to dose to water in order to properly compare both calculated dose distributions [9]. For this purpose, Siebers et al. [8] proposed a method based on the Bragg-Gray cavity theory, where MC-based D_m are converted into D_w using average stopping power ratio for water to medium. Their study showed that the difference between D_m and converted D_w for a head and neck plan was in the order of 1–2% for soft tissues, whereas this difference could increase up to 10% in the presence of higher density materials, such as cortical bone. For prostate IMRT plans generated with 18 MV photon beams, Dogan et al. [10] stated that systematic dose errors of up to 8% may be introduced, when the hard bone structures are present and MC calculated D_m are converted to D_w using the method described in Siebers et al. [8].

Ma et al. [5] used the Monte Carlo method to verify IMRT dose distributions previously computed by the Corvus TPS, employing a finite-size pencil beam algorithm. In their work, they also investigated the dosimetric effect of the conversion of calculated dose to different materials for a vertebra IMRT dose plan delivered with photon beams of 15 MV. For this purpose, they compared the dose distributions calculated for different materials with different densities, as well as those calculated for water-equivalent-tissue with the corresponding densities. They reported differences of 2–3% between the dose to bone and the dose calculated in tissue with bone density. However, these

differences reached up to 10% for regions with hard bone, when the dose was converted using the stopping power ratio for tissue to bone following the method of Siebers et al. [8]. They concluded thus that the conversion using stopping power ratios may not be equivalent to MC dose calculated in tissue of variable densities.

Additional works published by Ma et al. [11,12] investigating the same subject showed differences $< 4\%$ between the doses calculated in different layered phantoms, including bone heterogeneity and those distributions calculated in the same phantoms, with the bone replaced by water of bone density. They also observed that the conversion of dose to bone to dose to water using the stopping power ratios resulted in differences higher than 10%. Similar discrepancies were also observed in dose distributions calculated in CT-based patient phantoms for an IMRT plan delivered with 15 MV photon beams.

In resume, there is some work on the conversion of D_m to D_w related to layered phantoms, as well as to patient phantoms irradiated by high-energy photon beams (>10 MV). In fact, most of these works devoted to IMRT treatments of prostate or vertebra regions were performed using photon beams with energy of 15 and 18 MV [10—12]. However, there are not similar studies performed for photon beams with lower energy, namely 6 MV. The use of low-energy photons (6 MV) for IMRT treatments has been extensively encouraged by several authors [13—15] and it remains a possible option for the delivery of prostate IMRT. The low-energy photon beams have shown to have certain advantage for IMRT plans over the high-energy photons (>10 MV), due to the negligible neutron contamination.

The purpose of the present work was to evaluate the effect of converting MC-based D_m *to* D_w for the verification of prostate IMRT dose distributions generated using 6 MV photon beams. IMRT plans were predicted by the Eclipse TPS using a pencil beam convolution algorithm, in which tissue heterogeneities are accounted for by a Modified Batho Power Law correction method. MC—IMRT plans were *simulated* using BEAMnrc code for each patient, and dose calculations were subsequently performed with the DOSXYZnrc code in real CT-based patient phantoms built with three different CT ramps: a conventional four material CT ramp and two simplified conversion ramps of air and water having different density configurations. The intercomparison between MC dose distributions allowed us to isolate the material composition effect from the density effect on the calculated doses. Our MC plans were also evaluated using the stopping power ratio method proposed by Siebers et al. [8] for the conversion of MC-based D_m to D_w.

Material and methods

Treatment planning

Dynamic or "sliding windows" IMRT treatment plans *for* 3 prostate cancer patients were generated with inverse planning using the Eclipse TPS (version 7.0). Patients were scanned in a supine position with a resolution of $0.0977 \times 0.0977 \times 0.3$ cm^3 using a Siemens CT scanner. Photon beams of 6 MV produced by a Varian 2100C/D linear accelerator equipped with a 120 — leaf Millenium MLC were used for treatment delivery. For all three plans, the treatment was divided into 3 different phases to produce a final prescribed dose of 76—78 Gy to the prostate and seminal vesicles, delivered in daily 2-Gy fractions. The first phase (Phase I) was planned to deliver 44 Gy to the volume PTV1 containing the prostate, lymph regional nodes, seminal vesicles and pelvic lymph nodes. In a second phase (Phase II), the MLC *opening* was reduced to conform the PTV2 (prostate, seminal vesicles and lymph regional nodes) for 10 Gy (patient 1 and 2) and 8 Gy (patient 3). In a last phase (Phase III), a total dose of 24 Gy was provided to the PTV3, including the prostate and the seminal vesicles.

For the IMRT plan used in Phase I, a seven-field (patients 1 and 3) and a five-field (patient 2) coplanar beam arrangement were applied with jaws field sizes of approximately 19×17 cm^2. For Phases II and III, the IMRT plan was composed of five coplanar fields (patient 1 and 2) and seven coplanar fields (patient 3), with average field sizes of 15×10 cm^2 and 12×10 cm^2, respectively.

The patient dose calculations were performed using a pencil beam convolution (PBC) algorithm, in which tissue heterogeneities *were* accounted for by a Modified Batho Power Law correction method [16]. The doses reported by these algorithms were calculated in water and subsequently corrected by the electron density, which is equivalent to calculate the dose using water with different electron densities.

Monte Carlo calculations

The Varian 2100C/D linear accelerator equipped with a 120-leaf Millenium MLC was accurately modeled for 6 MV photon beam using the BEAMnrc/EGSnrc user code [17,18]. The accelerator model consisted of several components, such as the target, primary collimator, vacuum exit window, flattening filter, monitor chamber, collimating jaws and the MLC.

The detailed geometry and dimensions of each component were set based on the manufacturer's specifications. A parallel circular electron beam hitting on the target with 6.2 MeV energy (monoenergetic) and a radius of 0.15 cm was chosen to match within 2%/2 mm the calculated depth dose and off—axis profiles in water with the experimental data measured with an ionization chamber (PTW 31002). The MLC device was fully modeled using the DYNVMLC model described by Heath et al. [19]. Due to the complex geometry considered in the MLC model, including rounded leaf and tongue and groove designs, this component was separately commissioned in order to verify the accuracy of the model [19,20]. The simulated dose profiles for a variety of MLC defined fields were compared to measurements carried out with radiographic films (EDR type) and ionization chamber (PinPoint model) in a homogeneous water phantom. The MLC model was able to reproduce effects, due to the leaf geometry (leakage, tongue and groove design and rounded leaf end design). The overall agreement was within less than 5% and 2% between calculations and film and ionization chambers measurements, respectively, for arbitrary fields shaped by the MLC. This agreement provided a good initial support for the use of this model as a tool for the verification of IMRT plans [21].

Monte Carlo simulations were split into three different stages. The first stage simulated the passage of the particles through the patient-independent part of the linac, i.e. up to a plane just upstream the secondary collimators or jaws (at 27.9 cm from the electron source). This step was performed only once with the resulting particle coordinate (energy, location, direction and particle type) scored in a phase-space file for subsequent use in the next step of the simulation. In the second stage, a set of output phase-space files for the various MLC and jaws field size configurations were obtained below the MLC, at 54 cm from the source. This stage is referred here as "patient-dependent" part, as it changed for each patient field configuration. Finally, the phase-space files scored in the second step were used as a source of the DOSXYZnrc code [22] to calculate dose distributions in the CT − based patient phantoms. For each patient, the plan information data, i.e. jaw positions, gantry angles and patient isocenter position, was exported from the clinical Eclipse TPS for MC simulations. Additionally, the position of the MLC leaves were directly read from the BEAMnrc code, using a leaf-sequence file exported previously from the TPS (an .mlc file).

Five hundred million electrons were incident upon the bremsstrahlung target, resulting in about 477 million photons at the phase-space plane location above the collimator jaws.

For the patient-dependent part, four independent runs (with different random number seeds) were simulated using the total number of particles scored in the previous stage (i.e. without recycling) for each beam of the treatment phases I and II. The resulting phase-space files for the 4 independent runs of a beam were then combined in a final phase-space file using the data analysis utility BEAMDP [23]. The combination of the phase-space files resulted in a final phase-space file with a large number of particles, while still retaining the characteristics (energy, angle, position, etc.) of the particles. For the beams of the phase I, the final phase-space files had between 2×10^7 and 7×10^7 particles, while, for the beams of the phase II, the files contained around 2×10^7 and 4×10^7 particles. The number of particles scored in the phase-space files was dependent on the size of the field defined by the jaws and the MLC for each beam arrangement. Using these final phase-space files, the individual beams for each phase of the treatment were simulated independently in the CT-based phantom. For that, the information of patient-dependent phase-space particles were used repeatedly (around 10−12 times) in the DOSXYZnrc-based calculations for both treatment phases.

The final dose distribution for each phase was the summation of the dose distributions from all individual beam arrangements. The average statistical uncertainty for the final distribution was less than 2%, in the regions of the targeted volumes (PTV and critical structures), and about 2.5% in the regions close to the confluence of the treatment beams. These statistics were considered sufficient for the dose analysis (DVH and dose distributions) based on the results reported by Keall et al. [24]. According to these authors, a statistical uncertainty of 2% has minimal effect on isodose levels, DVHs or biological indices.

The following transport parameters were set for the first two steps of the accelerator simulation: ECUT = AP = 700 keV, PCUT = AP = 10 keV, where AP and AE are the low-energy thresholds for the production of secondary bremsstrahlung and knock-on electrons, respectively; while ECUT and PCUT define the global cutoff energy for electron and photon transport, respectively. In order to improve the calculation efficiency, various variance reduction techniques were employed, such as uniform bremsstrahlung splitting with a photon splitting factor of 20, Russian Roulette and range rejection technique with ESAVE of 0.7 MeV in the bremmsstrahlung target and 1 MeV for the other accelerator components [18]. On the other hand, MC dose calculations in phantoms were carried out for ECUT and PCUT set to 0.521 MeV and 0.01 MeV, respectively. The value of the parameter ESTEPE (maximum fractional energy a charged particle can lose per step) was set to its default value of 25%. Phantoms were created via the DICOM RT toolbox [25] using the planning CT patient dataset as input. The conversion of CT numbers to materials and mass densities was handled by using several CT conversion ramps, as described in the next section. Finally, dose distributions were visualized in voxel phantoms using the visualization tool dosxyz_show included as part of the BEAM distribution [26].

The MC dose distributions normalized per unit of primary particles (Gy/part) (i.e. the amount of electrons colliding the target to produce photons) were converted into absolute dose distribution (Gy/UM), in order to compare to Eclipse TPS distributions. MC simulations of the linear accelerator were performed for the 6 MV photon beam under reference calibration conditions, i.e. a 10×10 cm^2 open field defined with jaws collimator at 100 cm SSD in an homogeneous water phantom. A conversion factor in Gy/UM was thus determined by the ratio of the maximum dose value obtained in the simulated central depth dose curve and the correspondent value experimentally measured with a cylindrical ionization chamber (0.125 cm^3 sensitive volume), under the same reference conditions. MC distribution for this procedure was calculated using DOSXYZnrc in a water phantom divided into 0.2 cm voxel along *X*, *Y* and *Z* axis. The statistical uncertainty of the MC dose value at the maximum depth was within 1%.

CT conversion ramps

MC phantoms were created using the planning CT patient dataset as input of the DICOM RT toolbox [24]. As previously mentioned, the original CT slices had a resolution of 512×512 and a pixel size of 0.0977 cm and were taken with a distance of 0.3 cm. MC simulations were performed in a reduced CT patient geometry, identical to that geometry used for TPS dose calculations, which did not include objects and air region positioned outside the patient contour. Additionally, the resolution of this reduced geometry was also set to the same resolution as the TPS, i.e. $0.25 \times 0.25 \times 0.3$ cm^3 in the *X*, *Y* and *Z* direction, respectively.

To build MC phantoms, three different ramps using a four material bin scheme were considered to convert CT data into material and mass density. The conventional CTCREATE/DOSXYZnrc [22] conversion ramp using four materials (air, lung, tissue and bone with the proper mass density) was considered (Fig. 1). We denote the MC phantom created using this CTCREATE ramp as "conventional phantom". A simplified CT ramp using air and water

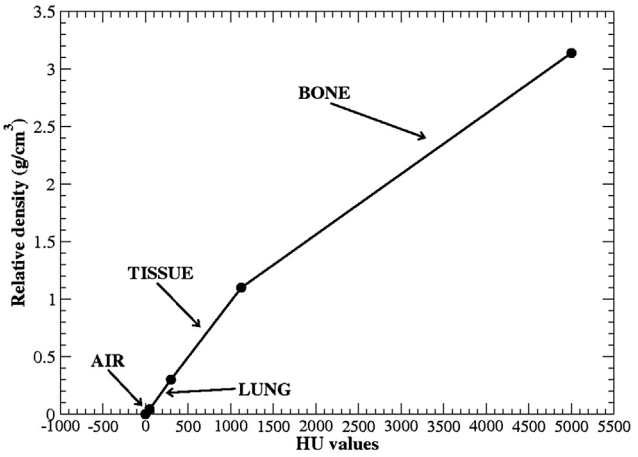

Figure 1 The CT ramp for the conversion of CT values to material type and densities according to the conventional CTCREATE ramp which uses four materials: air, lung, tissue and bone [22]. The density and composition of the material used in this ramp were the values included in the PEGS4 cross section data file.

of variable density (referred as "*water variable* ρ") was also used to build MC patient phantoms. For this conversion ramp, the cross sections of three materials, called as LUNG_WATER, TISSUE_WATER and BONE_WATER, were generated by the PEGS4 data-preprocessing code [12]. These new materials were defined as having the composition of water and the mass density of lung (ρ = 0.26 g cm^{-3}), tissue (ρ = 1.0 g cm^{-3}) and bone (ρ = 1.85 g cm^{-3}) materials considered in the conventional CT ramp. MC patient phantoms were also constructed using a second simplified ramp, referred as "*water unit* ρ", which considered only air and water with unit density. Table 1 summarizes the material intervals of the four bins used in each CT conversion procedure. MC—IMRT dose calculations for the three patients included in this study were performed in the three above referred phantoms using the DOSXYZnrc code, as described above in previous section.

Dose to medium to dose to water conversion

To explore the effect of the conversion of dose to medium to dose to water, the MC dose distributions D_m obtained in the phantom created using a conventional CT ramp were converted to dose to water (D_w) using the method proposed by [8]. This method is based on the Bragg-Gray cavity theory and provides a relation between D_w and D_m given by:

$$D_w = D_m S_{w,m}$$

where $S_{w,m}$ is the unrestricted water to medium mass collision stopping power ratio averaged over the energy spectra of primary electrons produced in photon interactions at the point of interest. Siebers et al. [8] assessed the dependence of $S_{w,m}$ on energy for the materials of the patient-like geometry and they found that $S_{w,m}$ varies less than 1% throughout the field for a given photon beam energy. Therefore, a single correction factor for each material was proposed to convert D_m to D_w for a given photon beam energy.

The conversion of the dose based on the previous relation can be accomplished using two different methods. On the one hand, the dose conversion may be performed in a post-processing step, based on the fact that $S_{w,m}$ is approximately invariant for patient-like materials throughout a photon radiation therapy field [8]. Alternatively, the conversion may be carried out during the execution of the particle transport on a track-by-track basis by multiplying the energy deposited in a voxel by the stopping power ratio [27]. This last method is done in the MC transport code, thereby directly obtaining D_w. As it has been previously shown by Siebers et al. [8], converting the dose in a post-processing step is valid for photon beams. In 2007, Gardner et al. [28] reported that the differences between the two methods were clinically insignificant in homogeneous phantoms ranging in density from 0.3 g cm^{-3} to 2.5 g cm^{-3}, in a bone-lung-bone phantom with steep density gradients, as well as in several prostate and head and neck patient cases. In the present work, the conversion from dose to medium to dose to water was carried out in a post-processing step using the DICOM RT — toolbox [25].

Results and discussion

Material composition and density effect on MC dose distributions

In this section, we present the MC dose distributions calculated in conventional and both simplified phantoms for 3 prostate IMRT plans (Phase I and II), in order to

Table 1 CT conversion ramps used to build Monte Carlo phantoms from the CT dataset of patients. The interval of mass density and corresponding CT number are illustrated in Fig. 1. The EGSnrc/521ICRU materials database was considered [17]. The materials LUNG_WATER, TISSUE_WATER and BONE_WATER were generated using the PEGS4 processor [17]. The low-energy thresholds for the production of knock-on electrons was set to AE = 0.521 MeV (total energy) and the threshold for bremsstrhalung events was set to AP = 0.010 MeV for all materials.

	CT conversion ramps		
Material interval	Conventional CTCREATE	"Water variable ρ"	"Water unit ρ"
1	AIR	AIR	AIR
2	LUNG	LUNG_WATER	WATER
3	TISSUE	TISSUE_WATER	WATER
4	BONE	BONE_WATER	WATER

evaluate the individual contributions of material composition and density to dose distributions.

Figure 2a shows the comparison of an X dose profile calculated for three MC phantoms which were created using the CT conversion ramps summarized in Table 1. The profile was plotted through the transversal CT slice containing the isocentre ($z = -0.1734$ cm) for the treatment phase II of patient 1 (Fig. 2b). The exact position of the profile is indicated by the horizontal white lines in Fig. 2b. The gray highlighted region in Fig. 2a represents the extent of bony regions situated along the profile axis.

As shown in this figure, the differences between the profiles calculated in water with variable densities and the profiles calculated in water with unit density were found less than 1% in all regions, including those regions containing bone. This fact indicates that differences in mass density of the water do not affect significantly the MC dose distributions. On the other hand, it is seen that the dose calculated in both simplified water phantoms shows

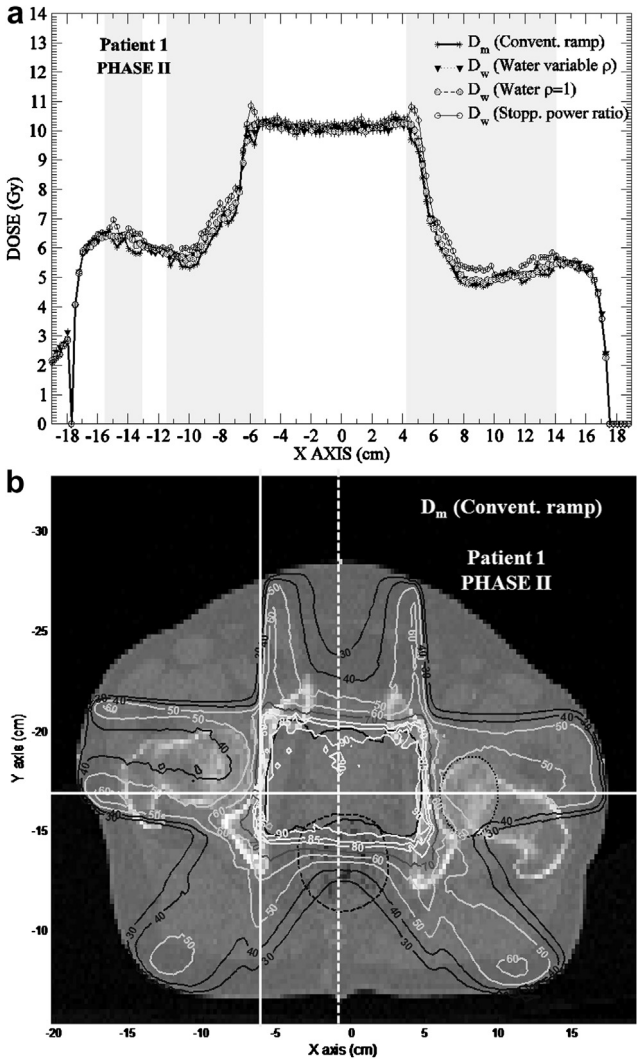

Figure 2 (a) Comparison of dose profiles calculated along the *X* axis for MC phantoms built using conventional (CTCREATE) and simplified CT ramps ("*water variable ρ*" and "*water unit ρ*"). Profiles were taken at the position $y = -16.13$ cm of the transversal CT image slice (b), which contain the isocenter ($z = -0.1734$ cm) for the Phase II of the IMRT treatment of patient 1. The horizontal white lines in the CT image indicate the position where the profile is plotted. MC dose profile D_m (Convent. ramp) converted using the stopping power ratios for water to medium is also presented. The isodose lines are given as 30, 40, 50, 60, 70, 80 and 90% of the maximum dose of this case (10.95 Gy). Black lines on CT image indicate the PTV volume (continuous line) and both rectum and left femoral head (dashed line).

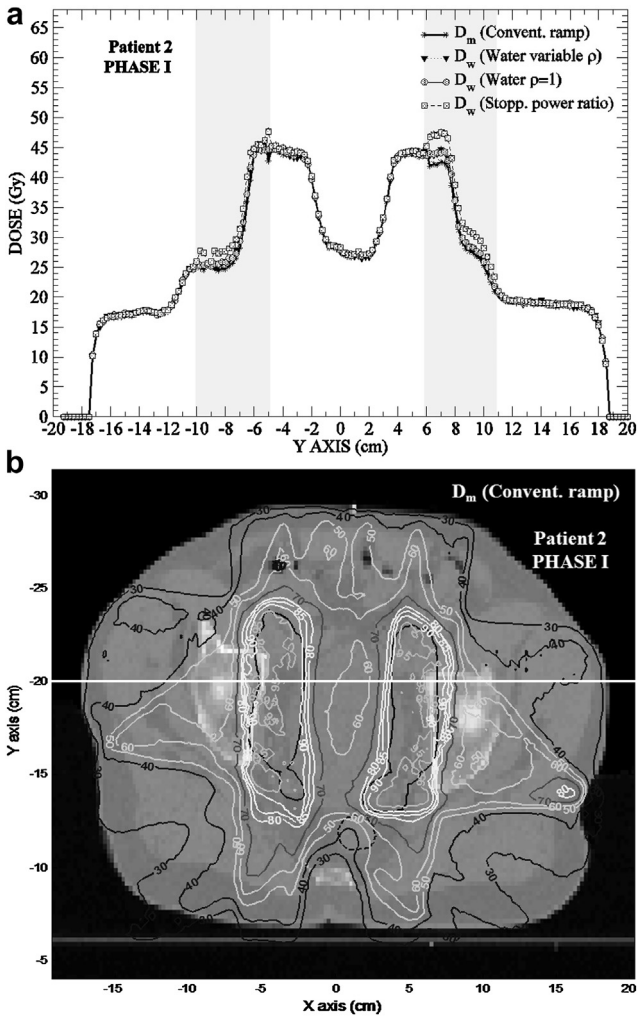

Figure 3 (a) Comparison of dose profiles calculated along the *X* axis for MC phantoms built using conventional (CTCREATE) and simplified CT ramps ("*water variable ρ*" and "*water unit ρ*"). Profiles were taken at the position $y = -20$ cm of the transversal CT image slice (b), which contain the isocenter ($z = 4.8328$ cm) for the phase I of the IMRT treatment of patient 2. The horizontal white lines in the CT image indicate the position where the profile is plotted. MC dose profile D_m (Convent. ramp) converted using the stopping power ratios for water to medium is also presented. The isodose lines are given as 30, 40, 50, 60, 70, 80 and 90% of the maximum dose of treatment (46.44 Gy). Represented volumes on CT image are PTV volume (black continuous line) and rectum (black dashed line).

differences of about 4%, with the dose values calculated using the conventional phantom in regions close to bones. The cause of these discrepancies may be partially explained by the effect of the bone media (high atomic number and high density), which was accurately accounted by MC dose calculations performed in conventional phantoms, but not in both simplified water phantoms.

Similar observations were made for dose profiles within the other patients included in this study, as shown in Fig. 3a for patient 2. This figure illustrates the comparison of dose profiles calculated with MC in conventional and simplified phantoms in a transversal slice through the respective isocenter, in positions where bony regions are presented.

Figure 4 presents the comparison of dose profiles for the same MC phantoms as in Fig. 2, but in this case such profiles were plotted along the *Y* axis at two different positions of the CT slice (Fig. 2b). In Fig. 4a, a profile was plotted in a region adjacent to the femoral heads, whereas the profile illustrated in Fig. 4b was calculated through a region containing less bone structures. The positions of both profiles are represented by the vertical continuous and dashed white lines in Fig. 2(b), respectively. It is clear from Fig. 4a that the differences between dose profiles for the two simplified water phantoms, i.e. water with variable density and water with unit density, are also negligible as shown in the *X* profile. Larger discrepancies up to 4% are observed between the profiles calculated in medium (conventional phantom) and in water of unit and variable density. In Fig. 4b, it should be noted that, due to the lack of regions with bone found through this profile location, the observed differences between dose to medium and both dose to water with unit density and variable density are not significant (1%), when compared to previous *Y* profiles (Fig. 4a).

The MC dose profile calculated in medium (D_m), obtained using the conventional ramp to built the patient phantom, was converted to dose to water (D_w) using the stopping power ratios for water to medium, as described in the previous section. The converted dose profiles are also

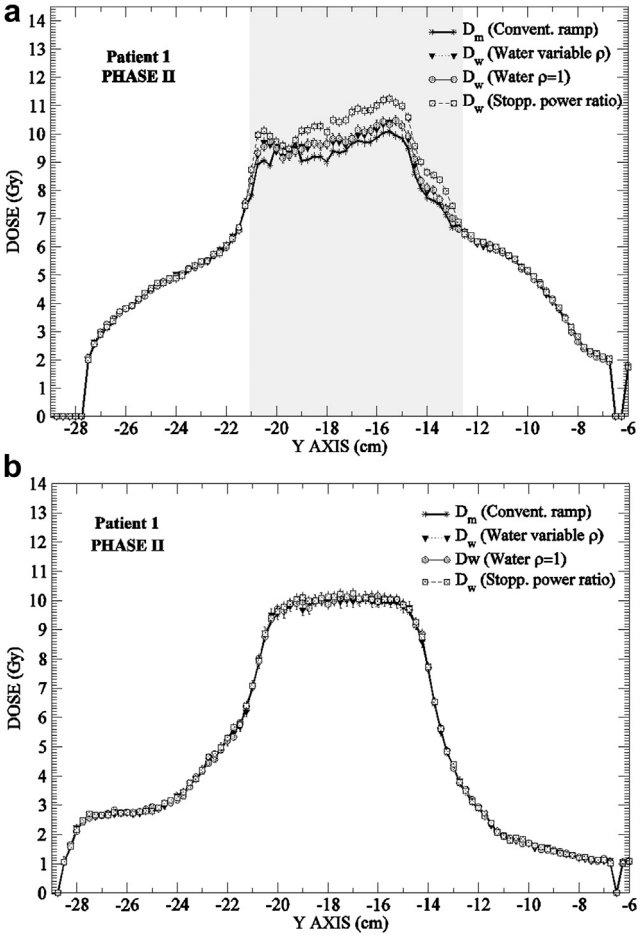

Figure 4 Comparison of dose profiles calculated along the *Y* axis for MC phantoms built using conventional (CTCREATE) and simplified CT ramps (*"water variable ρ"* and *"water unit ρ"*). Profiles were taken at the position (a) $x = -6.03$ cm (vertical continuous line) and (b) $x = -0.78$ cm (vertical dashed line) of the transversal CT image slice (Fig. 2(b)), which contain the isocenter ($z = -0.1734$ cm) for the phase II of the IMRT treatment of patient 1. MC dose profile D_m (Convent. ramp) converted using the stopping power ratios for water to medium is also shown.

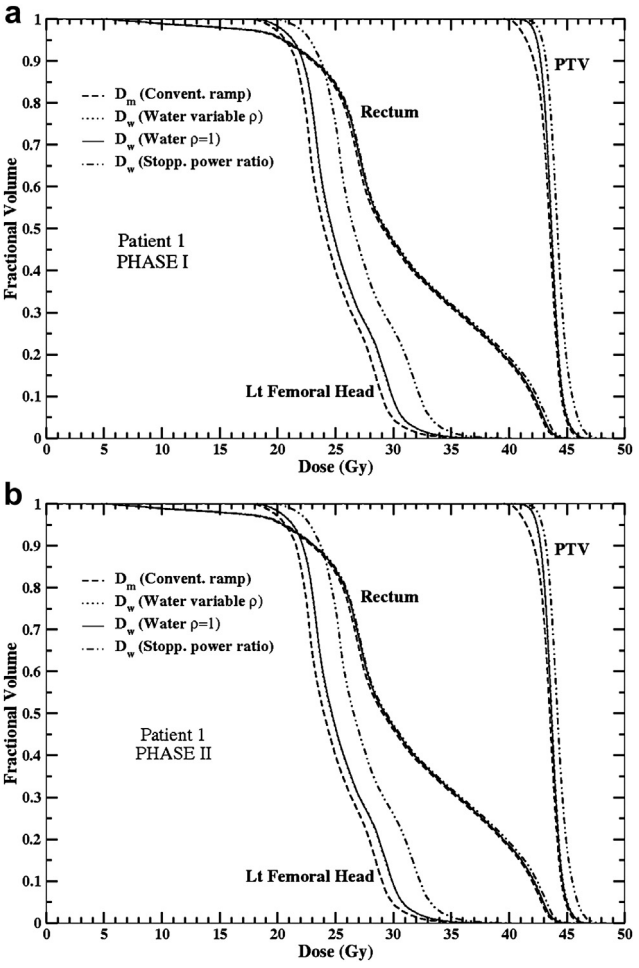

Figure 5 DVHs of the PTV, rectum and left femoral head calculated by MC in patient phantoms built using different CT conversion ramps (Table 1) for the phase I (a) and II (b) of patient 1. DVH for the D_m (Convent. ramp) distribution converted to dose to water using stopping power ratio is also shown.

included in previous Figs. 2—4. Comparing the dose to medium and the converted D_w dose profiles, it is clear from Fig. 4a that the conversion of dose with stopping power ratios increases about 9% the dose D_m in the femoral heads regions (bony structures), while it does not affect the dose in the tissue surrounding these regions. The cause of this increase in the bone areas can be mainly due to the high mass stopping power ratio $S_{w,m}$ for bone (1.114 for 6 MV photon beam), compared to the value for tissue (1.01 for 6 MV photon beam). These results are consistent with the previous results published by Ma et al. [11,12].

The dosimetric effect caused by differences in the materials used in MC phantoms was also evaluated through the dose-volume histogram (DVH) curves. Figure 5 illustrates the comparison of DVHs calculated by Monte Carlo for the phantoms constructed using the CT ramps of Table 1. The DVHs of target volumes (PTV) and two critical structures (left femoral head and rectum) are displayed for the phase I (Fig. 5a) and II (Fig. 5b) of the patient 1. As seen, there are no significant differences between the DVH of the PTV calculated using a conventional ramp and both simplified ramps with water for both treatment phases. Conversely, discrepancies of 3% are observed between DVHs of the femoral heads for the MC phantoms created using the conventional CT ramp and those created with both simplified CT ramps. Additionally, it is also noted in Fig. 5 that there is a significant shift by about 6% in the DVH of the femoral heads for the plan that was calculated using water of variable densities, compared to the plan converted from medium (conventional ramp) to water using the stopping power ratio method. However, the DVHs of the PTV are not affected by the conversion of D_m to D_w for both treatment phases. These results confirm the tendency observed previously in the dose profiles (Figs. 2—4).

The comparison of rectum DVHs calculated in conventional and simplified phantoms does not show significant differences (1%). This could be mainly explained because the air was defined with the same composition and density for all three CT ramps used in this study (Table 1).

Eclipse pencil beam convolution and MC dose comparison

The discrepancies between IMRT plans calculated with MC simulations and predicted by Eclipse system (PBC algorithm) were evaluated in terms of isodose distributions and DVHs of the target (PTV), rectum and left femoral head structure. Figure 6a—c compares isodose distributions

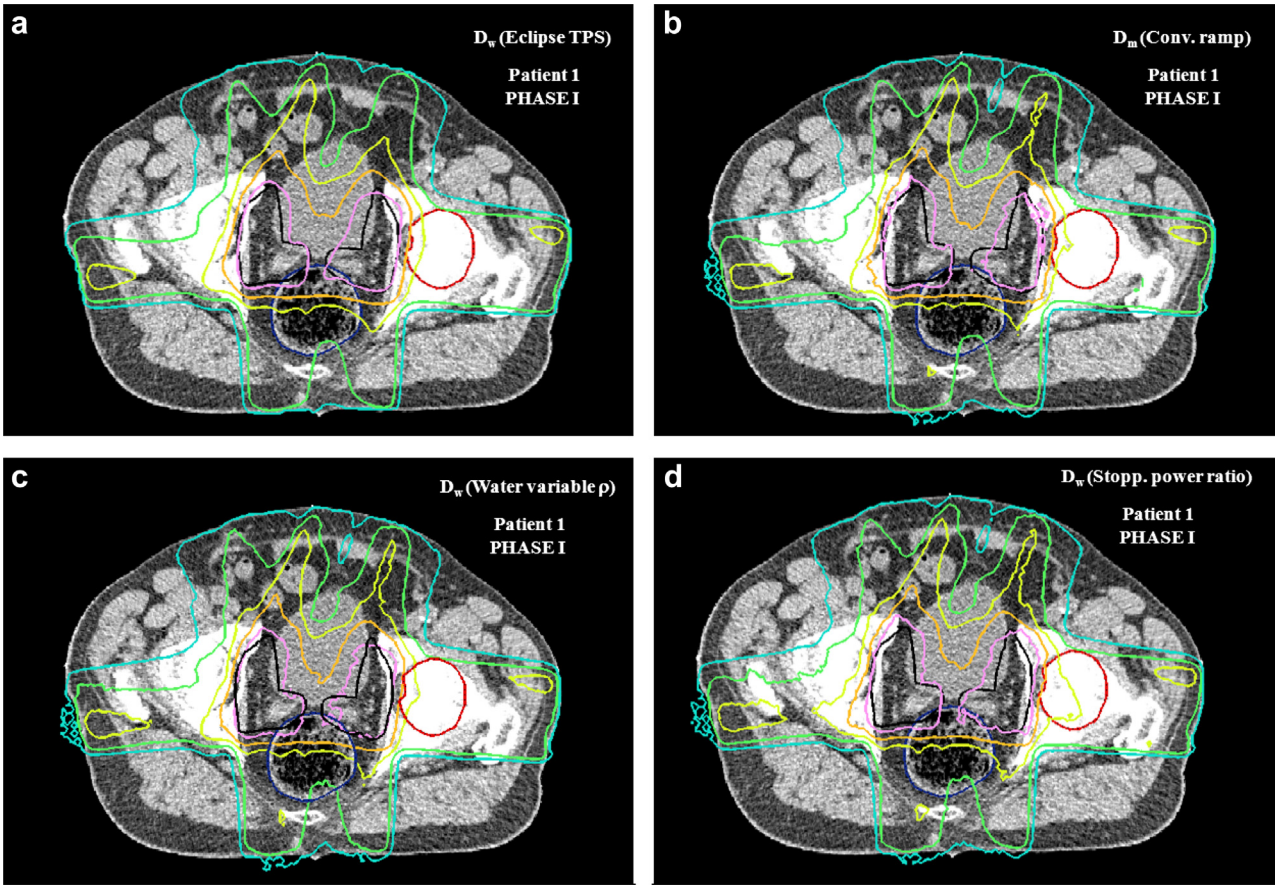

Figure 6 Comparison of isodose distribution for the phase I of the IMRT treatment in patient 1 calculated by Eclipse TPS using a PBC algorithm (a) and by Monte Carlo using: (b) a conventional phantom (D_m), (c) simplified water phantom of water with variable density (D_w) and (c) converted D_m to D_w with stopping power ratio. The isodose lines are 13.9(blue), 20.9(green), 27.87(yellow), 34.84(orange) and 41.81 Gy(pink). Represented volumes on CT images are PTV volume (black), rectum (blue) and left femoral head (red). (For interpretation of the references to color in this figure legend, the reader is referred to the web version of this article.)

obtained from the Eclipse system with Monte Carlo simulations performed in conventional phantoms (D_m) and in simplified phantom of water with variable density (D_w) for the Phase I of the IMRT plan in patient 1. Moreover, the isodose curves from Monte Carlo simulations, calculated in medium and converted to dose to water using stopping power ratios, are illustrated in Fig. 6d. It is seen in Fig. 6 that the MC dose distributions (conventional and simplified phantoms) in the target show a good agreement (about 2%) with Eclipse *PBC*. In the regions including heterogeneities (air and bone), differences up to 3—4% could be observed between the Eclipse *PBC* calculations and the Monte Carlo simulation in the conventional phantom. In the bone regions, large differences (6%) in isodose curves were observed between MC simulations and the Eclipse *PBC calculations*, when the MC distributions were converted to dose to water using the stopping power ratios. As seen in Fig. 6a and d, the 27.87 Gy line (light green line) varied noticeably between these two dose distributions within the region of the left femoral head (region limited by the red line).

DVH curves *for* the Eclipse *PBC algorithm* were compared with DVHs calculated using Monte Carlo in the different phantoms above described for the phase I and II of patient 1 and 2, as shown in Fig. 7. DVHs for the MC dose distribution converted from medium to water using stopping power ratio are also shown in the figures. For all cases, the target DVHs calculated using Monte Carlo simulations (all phantoms) agreed within 1% with the DVHs calculated by the *PBC algorithm*. For femoral heads, discrepancies by about 3% were found in the DVH computed by the Eclipse *PBC* as compared with Monte Carlo calculations in medium (conventional phantom). The conversion of MC dose distributions from D_m to D_w results in a difference of about 6% when compared to the TPS for the femoral structure. For the target, however, the DVHs of converted dose distributions do not show such large differences when compared with the Eclipse system.

For the rectum, the DVHs curves *for* the Eclipse *PBC algorithm* for patient 1 show a good agreement (2%) with the DVH curves calculated using MC simulations in medium and those converted from medium to water. For the patient

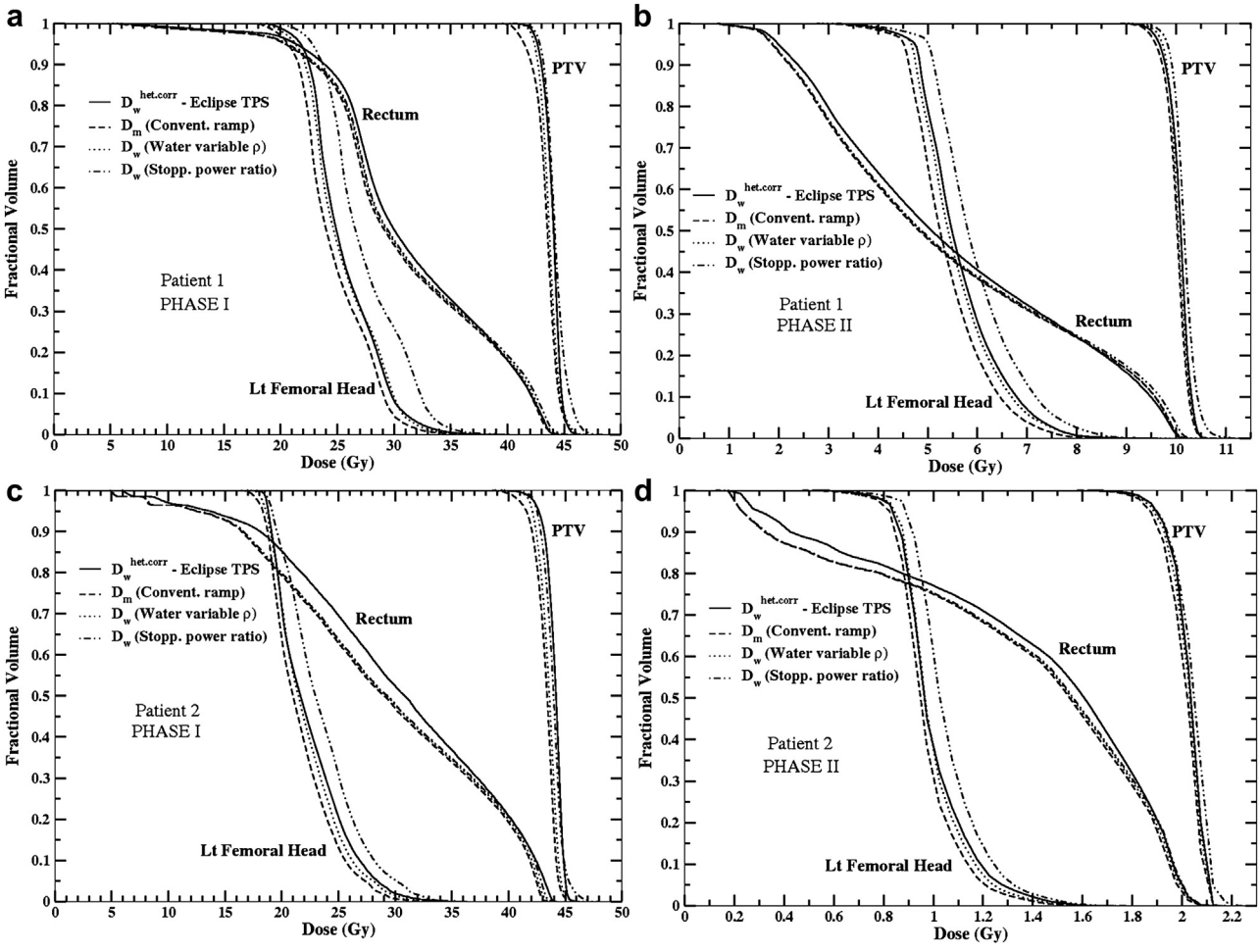

Figure 7 Comparison of DVH curves calculated by Eclipse TPS using a PBC algorithm (continuous line) and by Monte Carlo (dashed lines) for the PTV, rectum and the left femoral head. Monte Carlo calculations were performed in phantoms built with a conventional CT ramp and the simplified CT ramp of water of variable densities. DVH for the D_m distribution converted from dose to medium to dose to water using stopping power ratio is also shown. DVHs are illustrated for phase I (a—c) and II (b—d) of patient 1 and 2.

2, it can be seen that the Eclipse *PBC calculations* estimate a higher dose, up to 5—6%, than both MC dose values calculated in medium and those converted from medium to water using the stopping power ratios, in particular for the range of low doses.

Similar findings for DVHs were observed within patient 3 (not shown).

Conclusions

The dose distributions of three IMRT plans of prostate patients planned by Eclipse TPS with 6 MV photon beams were evaluated using MC calculation method. The initial plans were computed by the Eclipse system using a Pencil Beam Convolution algorithm with a Modified Batho Power Law heterogeneity correction. The plans were subsequently recalculated using DOSXYZnrc code in MC conventional and simplified CT-based phantoms. Conventional phantoms were created from CT patient data using a conventional four material ramp (CTCREATE) to convert CT numbers into material and mass density. Simplified phantoms were created using simplified ramps: air and water with variable density, as well as air and water with unit density.

The individual contribution of material properties (composition and density) used in MC phantoms to dose was investigated for these plans. The effect of the elemental composition of materials was found to be less than 1% on dose profiles and DVHs of soft tissue. This effect increased up to 3% in regions where bone structures such as the femoral heads. On the other hand, the mass density of materials of the MC phantoms did not show a significant influence (about 1%) on dose profiles and DVHs for all tissues.

The conversion of MC dose distributions from medium to water using the stopping power ratios [8] introduced an increase of about 9% in DVHs of bony structures, such as femoral heads. In contrast, such dose conversion did not affect significantly (1%) the dose in soft tissues and critical structures containing air, such as the rectum.

The isodose comparison between Eclipse *PBC calculations* and MC simulations in conventional phantoms showed a good agreement (2%), except for heterogeneous regions containing bone and air (femoral heads or rectum structures), where differences of up to 4% were observed. This finding was confirmed by the DVH comparison, where Monte Carlo calculations performed in conventional phantoms presented discrepancies of 1% and 3—6% with *PBC* for the PTV volumes and for critical structures (femoral head and rectum), respectively.

A good agreement was reached between dose distributions predicted by the Eclipse *PBC algorithm* and those calculated with MC in simplified phantoms of air and water with variable densities. Using these simplified phantoms, differences of about 1% were found in the DVHs of target, femoral heads and rectum compared to *PBC*. On the other hand, after converting MC doses from medium to water with the stopping power ratios, DVH of MC calculated distributions for femoral heads became up to 6% higher than the one predicted by the *Eclipse PBC* distributions.

For the rectum, the Eclipse *PBC algorithm* may estimate a higher dose (up to 6%) in the DVH than the MC dose calculated in medium D_m, as well as D_m converted to water using the stopping power ratios. This overestimation is more significant for the treatment plans considering a high number of fields (3 posterior fields) to irradiate the rectum region.

In conclusion, MC calculations using a simplified CT ramp of water with variable density lead to results very close (3%) to the most precise MC calculations including all different media. Consequently, it can be concluded that *Eclipse PBC* algorithms computing doses using water with different densities provide values close to doses to different media as computed by MC algorithms.

In order to follow the AAPM TG 105 recommendations to convert MC dose results from media to water, our results show that, for prostate IMRT plans delivered with 6 MV photon beams, no conversion of MC dose from medium to water using stopping power ratio is needed. In contrast, MC dose calculations using water with variable density may be a simple way to solve the problem found by using the dose conversion method [8].

Acknowledgments

This work was supported by grant SFRH/BD/28918/2006 from Fundação para a Ciência e a Tecnologia.

References

[1] Guckenberger M, Flentje M. Intensity-modulated radiotherapy (IMRT) of localized prostate cancer. Strahlenther Onkol 2006; 2:57—62.
[2] Intensity Modulated Radiation Therapy Collaborative Working Group. Intensity-modulated radiotherapy: current status and issues of interest. Int J Radiat Oncol Biol Phys 2001;51: 880—914.
[3] Low DA, Moran JM, Dempsey JF, Dong L, Oldham M. Dosimetry tools and techniques for IMRT. Med Phys 2011;38:1313—38.
[4] Ma CM, Jiang SB, Pawlicki T, Chen Y, Li JS, Deng J, et al. A quality assurance phantom for IMRT dose verification. Phys Med Biol 2003;48:561—72.
[5] Ma CM, Pawlicki T, Jiang SB, Li JS, Deng J, Mok E, et al. Monte Carlo verification of IMRT dose distributions from a commercial treatment planning optimization system. Phys Med Biol 2000;45:2483—95.
[6] Ma CM, Li J, Pawlicki T, Jiang S, Deng J, Lee M, et al. Monte Carlo dose calculation tool for radiotherapy treatment planning. Phys Med Biol 2002;47:1671—89.
[7] Leal A, Sánchez-Doblado F, Arráns R, Roselló J, Carrasco Pavón E, Lagares JF. Routine IMRT verification by means of an automated Monte Carlo simulation system. Int J Radiat Oncol Biol Phys 2003;56:58—68.
[8] Siebers JV, Keall PJ, Nahum AE, Mohan R. Converting absorbed dose to medium to absorbed dose to water for Monte Carlo based photon beam dose calculations. Phys Med Biol 2000;45: 983—95.
[9] Chetty IJ, Curran B, Cygler JE, DeMarco JJ, Ezzell G, Faddegon BA, et al. Report of the AAPM task group no. 105: issues associated with clinical implementation of Monte Carlo-based photon and electron external beam treatment planning. Med Phys 2007;34:4818—53.
[10] Dogan N, Siebers JV, Keall PJ. Clinical comparison of head and neck and prostate IMRT plans using absorbed dose to medium and absorbed dose to water. Phys Med Biol 2006;51:4967—80.

[11] Ma CM, Li JS. Monte Carlo dose calculation for radiotherapy treatment planning: dose to water or dose to medium?. IFMBE proceedings, vol. 25/I; 2009. pp. 326—329.
[12] Ma CM, Li J. Dose specification for radiation therapy: dose to water or dose to medium? Phys Med Biol 2011;56:3073—89.
[13] De Boer SF, Kumek Y, Jaggernauth W, Podgorsak MB. The effect of beam energy on the quality of IMRT plans for prostate conformal radiotherapy. Technol Cancer Res Treat 2007; 6:139—46.
[14] Welsh JS, Mackie TR, Limmer JP. High-energy photons in IMRT: uncertainties and risks for questionable gain. Technol Cancer Res Treat 2007;6:147—9.
[15] Thangavelu S, Jayakumar S, Gavindarajan KN, Supe SS, Nagrajan V, Nagarajan M. Influence of photon energy on the quality of prostate intensity modulated radiation therapy plans based on analysis of physical indices. J Med Phys 2011; 36:29—34.
[16] Sontag MR, Cunningham JR. Corrections to absorbed dose calculations for tissue inhomogeneities. Med Phys 1977;4: 431—6.
[17] Kawrakow I, Mainegra-Hing E, Rogers DWO, Tessier F, Walters BRB. The EGSnrc code system: Monte Carlo simulation of electron and photon transport. NRCC report PIRS; 2010. 701.
[18] Rogers DWO, Walters B, Kawrakow I. BEAMnrc users manual. NRCC report PIRS; 2009. 0509(A) revK.
[19] Heath E, Seuntjens J. Development and validation of a BEAMnrc component module for accurate Monte Carlo modelling of the varian dynamic millenium multileaf collimator. Phys Med Biol 2003;48:4045—63.
[20] Jang SY, Vassiliev ON, Liu HH, Mohan R, Siebers JV. Development and commissioning of a multileaf collimator model in Monte Carlo dose calculations for intensity-modulated radiation therapy. Med Phys 2006;33:770—81.
[21] Zarza-Moreno M, Mateus D, Varelas I, Pontes M, Souto AC, Borges C, et al. Assessment of the Multileaf Collimator characteristics for Monte Carlo modeling of Intensity Modulated Radiotherapy. Proceedings of the 16th National Conference of Physics (Lisbon, Portugal) 2008; p 153. (private communication).
[22] Walters B, Kawrakow I, Rogers DWO. DOSXYZnrc users manual. Report; 2005. PIRS 794revB.
[23] Ma CM, Rogers DWO. BEAMDP users manual. NRCC report; 2009. PIRS-0509(C) revA.
[24] Keall PJ, Siebers JV, Jeraj R, Mohan R. The effect of dose calculation uncertainty on the evaluation of radiotherapy plans. Med Phys 200; 27: 478—484.
[25] Spezi E, Lewis DG, Smith CW. A DICOM-RT-based toolbox for the evaluation and verification of radiotherapy plans. Phys Med Biol 2002;47:4223—32.
[26] Kawrakow I. The dose visualization tool dosxyz_show. NRCC report PIRS; 2007. 0624.
[27] Kawrakow I and Fippel M. VMC++, electron and photon Monte Carlo calculations optimized for radiation treatment planning advanced Monte Carlo for radiation physics, particle transport simulation and applications: Proc. Monte Carlo 2000 meeting (Lisbon) pp. 229—236.
[28] Gardner JK, Siebers JV, Kawrakow I. Comparison of two methods to compute the absorbed dose to water for photon beams. Phys Med Biol 2007;52:N439—47.